RSC Advances

PAPER

View Article Online
View Journal | View Issue

Cite this: *RSC Adv.*, 2024, **14**, 11098

Synthesis of novel bioactive pyrido[2,3-*d*] pyrimidine derivatives with potent cytotoxicity through apoptosis as PIM-1 kinase inhibitors†

Eman S. Tantawy,[a] Mohamed S. Nafie,[*bc] Hesham A. Morsy,[d] Hassan A. El-Sayed,[a] Ahmed H. Moustafa[a] and Samar M. Mohammed[a]

Received 4th February 2024
Accepted 30th March 2024

DOI: 10.1039/d4ra00902a

rsc.li/rsc-advances

Direct synthesis and cytotoxicity activity of new series of pyrido[2,3-*d*]pyrimidine was described. Nicotinamide **2** was synthesized *via* cyclization of *N*-cyclohexyl derivative with cyanoacetamide. The *o*-aminonicotinonitrile **2** was subjected to acylation or thio acylation process followed by intramolecular heterocyclization to afford the desired pyrido[2,3-*d*]pyrimidine (**3–10**) and pyrido triazine **11**. Compounds **4** and **11** exhibited remarkable cytotoxicity against MCF-7 cells with IC_{50} values of 0.57 μM and 1.31 μM and IC_{50} values of 1.13 μM and 0.99 μM against HepG2 cells. Interestingly, compounds **4** and **10** had potent PIM-1 kinase inhibition with IC_{50} values of 11.4 and 17.2 nM, respectively, with inhibition of 97.8% and 94.6% compared to staurosporine (IC_{50} = 16.7 nM, with 95.6% inhibition). Moreover, compound **4** significantly activated apoptosis in MCF-7 cells, increasing the cell apoptosis by 58.29-fold by having 36.14% total apoptosis in treated cells compared to 0.62% for control. Moreover, it arrested the cell cycle at the G1 phase. PIM-1 kinase inhibition was virtually elucidated by the molecular docking study, highlighting binding interactions of the lead compound 4 towards the PIM-1 protein. Accordingly, compound **4** was validated as a promising PIM-1 targeted chemotherapeutic agent to treat breast cancer.

1 Introduction

Cancer is among the worst diseases that people face today. It ranks as the world's second-leading killer.[1,2] Cancer ranks high among the leading causes of mortality on a global scale, according to global statistics.[3,4] Modern medicine increasingly relies on medicinal chemists to identify targeted chemotherapy drugs.[5,6] By binding to specific molecular targets, these medications cause severe damage to cancer cells, therefore inhibiting their proliferation.[7,8] Because of their many biological uses, pyridine nuclei are significant nitrogen-containing heterocyclic systems. Important biological processes include anticancer,[9] anti-Alzheimer's disease,[10] antibacterial,[11] antitubercular,[12] antifungal,[13] anti-inflammatory[14] activities, and the management of several cardiovascular disorders, including hypertension and angina.[15] In addition, pyridine derivatives were shown to halt the proliferation of human MCF-7 and HepG-2 cancer cells by increasing JNK levels and causing G2/M phase arrest *via* a p53–p21-driven pathway. Among the many well-known pharmacophores in medicinal chemistry are pyridopyrimidines and other bicyclic nitrogen-containing heterocyclic compounds. A great deal of research has focused on pyrido[2,3-*d*]pyrimidines. There have been reports of their anticonvulsant, antibacterial, anticancer, antipyretic, and analgesic properties. PIM-1 is highly expressed in many different types of cancer and has an impact on carcinogenesis, cell cycle progression, cell proliferation, cell death, and cell migration, making it a promising target for the development of new cancer drugs. The phosphorylation and regulation of several proteins involved in cell survival, proliferation, and apoptosis are crucial functions of PIM-1 kinase, which is why it is associated with numerous cancer forms.[16] It has been shown to be excessively expressed in numerous forms of solid tumors such as prostate as well as hematological malignancy such as leukemia, multiple myeloma, and diffuse large B cell lymphomas (DLBCL).[17] Fig. 1 shows a number of pyridine and pyridopyrimidine (**I–IV**) compounds that have potent anticancer effects, and it also includes some of our earlier publications on cyanopyridine-based compounds that have been demonstrated to be effective PIM-1 kinase inhibitors that induce cell death.[18–20]

Accordingly, new series of pyridines and pyridopyrimidines were rationally designed and synthesized, as highlighted Fig. 2, where the three pharmacophoric regions of lipophilic, hydrophilic moieties with the main scaffold of pyridopyrimidine were

[a]*Department of Chemistry, Faculty of Science, Zagazig University, Zagazig 44519, Egypt*

[b]*Department of Chemistry, College of Sciences, University of Sharjah, P. O. 27272, Sharjah, United Arab Emirates. E-mail: mohamed.elsayed@sharjah.ac.ae*

[c]*Chemistry Department, Faculty of Science, Suez Canal University, P. O. 41522, Ismailia, Egypt. E-mail: mohamed_nafie@science.suez.edu.eg*

[d]*Higher Institution of Engineering & Modern Technology, Elmarg, Cairo, 13774, Egypt*

† Electronic supplementary information (ESI) available: Spectroscopic characterizations of the synthesized compounds. See DOI: https://doi.org/10.1039/d4ra00902a

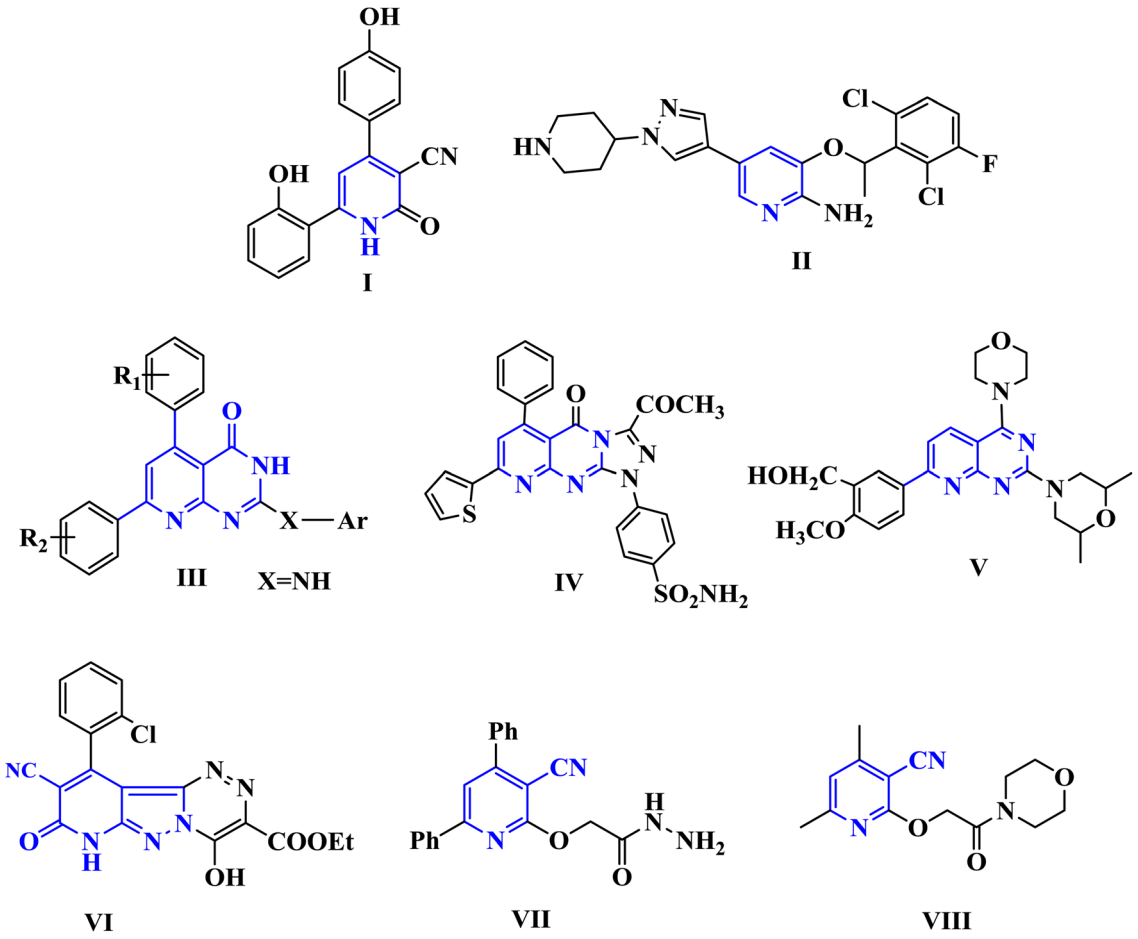

Fig. 1 Biologically active pyridine and pyridopyrimidines containing anti-cancer agents (I–V) and cyanopyridine-based compounds (VI–VIII) as PIM-1 kinase inhibitors.

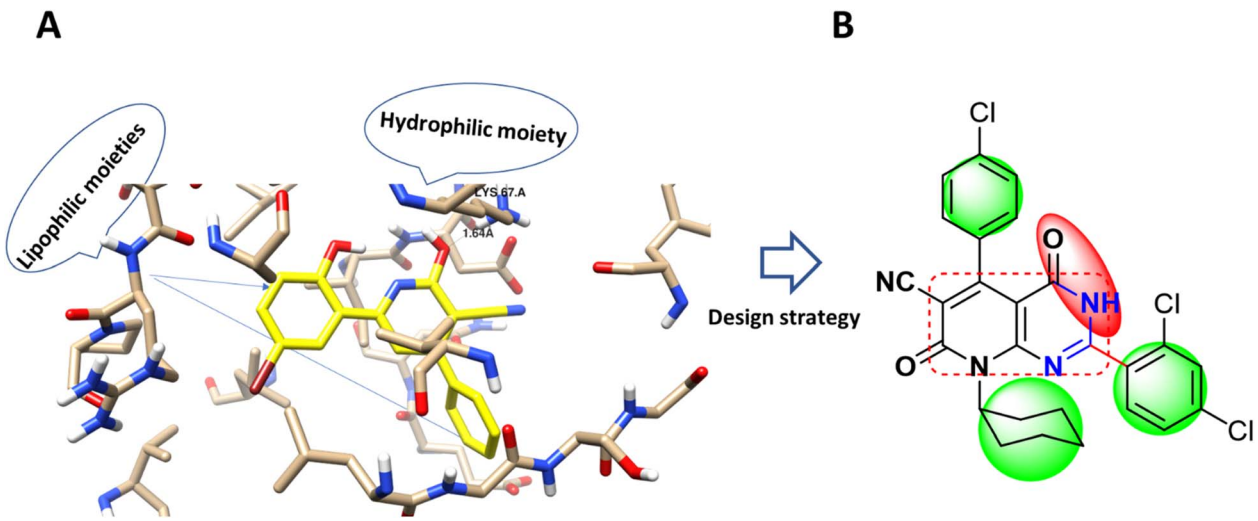

Fig. 2 (A) Molecular modeling of PIM-1 binding site (PDB 2OBJ) and the interaction pose with the co-crystallized ligand as a cyano-pyridine derivative (yellow-colored). (B) Design strategy of the target compound with the anchored pharmacophoric groups; lipophilic moiety (green) and hydrophilic (red) with the main scaffold (square circled).

highlighted. It was our intention to synthesize new derivatives with the same scaffold and different incorporated derivatives and to assess the anticancer activity of new substituted pyridine and pyridopyrimidines derivatives for more effective and target-oriented chemotherapeutics, as well as to study their molecular target, cytotoxicity, and cell death mechanism in both *in situ* and *in vitro* studies.

It was reported that incorporating pyridine derivatives exhibited potent anticancer activity against cancer cell lines such as HepG2 and MCF-7.[10]

2 Material and methods

2.1. Chemistry

All melting points were uncorrected and were measured using an Electrothermal IA 9100 apparatus. The IR spectra (KBr discs) were recorded on a Pye Unicam Sp-3-300 or a Shimadzu FTIR 8101 PC infrared spectrophotometer "Cairo University, Cairo, Egypt". The operation frequency was 400 MHz for ^{1}H NMR and 100 MHz for ^{13}C NMR using BRUKER 400 MHz spectrometer at Zagazig University, Faculty of Science, Zagazig, Egypt "Nucleic Acid Center Research". Elemental analyses were determined using PerkinElmer 240 "Cairo University, Cairo, Egypt". The coupling constants (J) are given in hertz. The chemical shifts are expressed on the δ (ppm) scale using TMS as the standard reference.

3-(4-Chlorophenyl)-2-cyano-*N*-cyclohexylacrylamide (**1**) was synthesized as reported method.[21] Mp = 178–180 °C. yield 95% [reported mp = 169–170 °C].

2.1.1. 2-Amino-4-(4-chlorophenyl)-5-cyano-1-cyclohexyl-6-oxo-1,6-dihydropyridine-3-carboxamide (2). A mixture of compound **1** (0.01 mol) and cyanoacetatamide (0.01 mol) in absolute ethanol (25 mL) and piperidine (5 drops) was heated under reflux for 18 h. The reaction mixture was cooled, and the obtained solid was filtrated off and washed with ethanol 95%. White crystals (ethanol), mp = 348–350 °C. Yield 91%. IR (KBr) spectrum, ν, cm^{-1}: 3325, 3300 (2NH$_2$), 2210 (C≡N) and 1665, 1650, (2C=O, amide). ^{1}H NMR (DMSO-d_6), δ (ppm): 0.72–1.46 (m, 11H, H$_{cyclohexyl}$), 6.96 (s, 2H, NH$_2$, exchange with D$_2$O), 7.29 (d, 2H, J = 8.80 Hz, Ar–H), 7.51 (d, 2H, J = 8.80 Hz, Ar–H), 11.45 (s, 2H, NH$_2$, exchange with D$_2$O). ^{13}C NMR (DMSO-d_6), δ (ppm): 23.72, 25.04, 25.35, 32.10, 81.61, 116.3 (C≡N), 118.6, 128.4, 128.7, 129.9, 130.4, 132.8, 133.1, 160.9 and 166.0. Anal. calcd for $C_{19}H_{19}ClN_4O_2$ (370.83): C, 61.54; H, 5.16; N, 15.11. Found: C, 61.53; H, 5.14; N, 15.10.

2.1.2. General method for synthesis of pyrido[2,3-*d*]pyrimidine (3–5). To a cold solution of *N*-cyclohexyl pyridone **2** (0.01 mol) in pyridine (20 mL), the acid chloride (0.01 mol), namely, (benzoyl chloride; 2,4-dichlorobenzoyl chloride or 2-furoyl chloride) was added gradually. The reaction mixture was stirred at r.t. for 2 h (monitored by TLC). The mixture was diluted with water (20 mL), and the stirring was continued for an additional 30 min. The formed precipitate was filtered off and recrystallized from EtOH.

2.1.3. 5-(4-Chlorophenyl)-8-cyclohexyl-4,7-dioxo-2-phenyl-3,4,7,8-tetrahydropyrido[2,3-*d*]pyrimidine-6-carbonitrile (3). White powder, mp = 226–228 °C. Yield 59%. IR (KBr) spectrum, ν, cm^{-1}: 3279 (NH), 2211 (C≡N) and 1664 (2C=O, amide). ^{1}H NMR (DMSO-d_6), δ(ppm): 1.08–1.66 (m, 11H, H$_{cyclohexyl}$), 7.25 (d, 2H, J = 8.40 Hz, Ar–H), 7.32 (d, 2H, J = 8.48 Hz, Ar–H), 7.38 (m, 2H, Ar–H), 7.50 (t, 1H, J = 7.69 Hz, Ar–H), 8.17 (d, 2H, J = 8.40 Hz, Ar–H), 11.48 (s, 1H, NH, exchange with D$_2$O). Anal. calcd for $C_{26}H_{21}ClN_4O_2$ (456.92): C, 68.34; H, 4.63; N, 12.26. Found: C, 68.32; H, 4.64; N, 12.27.

2.1.4. 5-(4-Chlorophenyl)-8-cyclohexyl-2-(2,4-dichlorophenyl)-4,7-dioxo-3,4,7,8-tetrahydropyrido[2,3-*d*]pyrimidine-6-carbonitrile (4). Colorless crystals, mp = 166–168 °C. Yield 57%. IR (KBr) spectrum, ν, cm^{-1}: 3280 (NH), 2230 (C≡N) and 1698, 1676 (2C=O, amide). ^{1}H NMR (DMSO-d_6) δ (ppm): 1.08–1.71 (m, 11H, H$_{cyclohexyl}$), 7.08–7.95 (m, 7H, Ar–H), 11.60 (s, 1H, NH, exchange with D$_2$O). ^{13}C NMR (DMSO-d_6), δ (ppm): 23.72, 24.14, 25.38, 34.29, 85.10, 100.3, 104.7, 117.5 (C≡N), 127.9, 128.0, 128.7, 129.9, 133.4, 133.8, 135.2, 153.2, 155.3, 157.2, 159.7, 160.0, 162.3, 163.2. Anal. calcd for $C_{26}H_{19}Cl_3N_4O_2$ (525.81): C, 59.39; H, 3.64; N, 10.66. Found: C, 59.28; H, 3.60; N, 10.71.

2.1.5. 5-(4-Chlorophenyl)-8-cyclohexyl-2-(furan-2-yl)-4,7-dioxo-3,4,7,8-tetrahydropyrido[2,3-*d*]pyrimidine-6-carbonitrile (5). Off white powder, mp = 302–304 °C. Yield 54%. IR (KBr) spectrum, ν, cm^{-1}: 3310 (NH), 2208 (C≡N) and 1649 (br, 2C=O amide). ^{1}H NMR (DMSO-d_6) δ (ppm): 1.05–1.47 (m, 11H, H$_{cyclohexyl}$), 6.98 (s, 1H, H$_{furyl}$), 7.29–7.52 (m, 6H, Ar–H), 11.49 (s, 1H, NH, exchange with D$_2$O). ^{13}C NMR (DMSO-d_6), δ (ppm): 22.39, 24.13, 25.04, 31.88, 67.40, 117.6 (C≡N), 128.0, 128.3, 128.4, 128.6, 128.7, 129.9, 130.9, 131.5, 133.7, 135.3, 155.6, 160.8, 163.3, 166.9. Anal. Calcd for $C_{24}H_{19}ClN_4O_3$ (446.89): C, 64.50; H, 4.29; N, 12.54. Found: C, 64.59; H, 4.30; N, 12.49.

2.1.6. 2-(Chloromethyl)-5-(4-chlorophenyl)-8-cyclohexyl-4,7-dioxo-3,4,7,8-tetrahydropyrido[2,3-*d*]pyrimidine-6-carbonitrile (6). A mixture of nicotinamide **2** (0.01 mol) and chloroacetyl chloride (0.01 mol) in acetonitrile (15 mL) and pyridine (5 mL) was heated under reflux for 8 h. The reaction mixture was poured into crushed ice and the formed precipitate was filtered off. White powder (EtOH), mp > 300 °C. Yield 65%. IR (KBr) spectrum, ν, cm^{-1}: 3429 (NH), 2215 (C≡N) and 1665 (br, 2C=O, amide). ^{1}H NMR (DMSO-d_6) δ (ppm): 0.70–1.84 (m, 11H, H$_{cyclohexyl}$), 4.73 (s, 2H, CH$_2$), 7.49 (d, 2H, J = 8.28 Hz, Ar–H), 8.14 (d, 2H, J = 8.28 Hz, Ar–H), 11.88 (s, 1H, NH exchange with D$_2$O). Anal. calcd for $C_{21}H_{18}Cl_2N_4O_2$ (429.30): C, 58.75; H, 4.23; N, 13.05. Found: C, 58.64; H, 4.21; N, 13.10.

2.1.7. Ethyl 5-(4-chlorophenyl)-6-cyano-8-cyclohexyl-4,7-dioxo-3,4,7,8-tetrahydropyrido[2,3-*d*]pyrimidine-2-carboxylate (7). A mixture of *N*-cyclohexyl pyridone **2** (0.01 mol) with diethyl oxalate (0.01 mol) in the presence of (20 mL) DMF was refluxed for 3 h, after completion of the reaction (monitored by TLC). The reaction mixture was poured into crushed ice, and the formed precipitate was filtered off. Colorless crystals (EtOH), mp = 278–280 °C. Yield 56%. IR (KBr) spectrum, ν, cm^{-1}: 3271 (NH), 2223 (C≡N) and 1718, 1659, (3C=O ester and amide). ^{1}H NMR (DMSO-d_6), δ (ppm): 1.18 (t, 3H, ^3J = 5.72 Hz, CH$_2$C<u>H</u>$_3$), 1.29–1.79 (m, 11H, H$_{cyclohexyl}$), 4.37 (q, 2H, ^3J = 5.72 Hz, C<u>H</u>$_2$CH$_3$), 7.63 (d, 2H, J = 8.48 Hz, Ar–H), 7.93 (d, 2H, J = 8.48 Hz, Ar–H), 8.10 (s, 1H, NH, exchange with D$_2$O). Anal. calcd for $C_{23}H_{21}ClN_4O_4$ (452.89): C, 61.00; H, 4.67; N, 12.37. Found: C, 61.02; H, 4.70; N, 12.35.

2.1.8. 5-(4-Chlorophenyl)-8-cyclohexyl-2-ethoxy-4,7-dioxo-3,4,7,8-tetrahydropyrido[2,3-*d*]pyrimidine-6-carbonitrile (8). Compound **2** (0.01 mol) and triethylorthoformate (0.01 mol) were dissolved in acetic anhydride (25 mL) and heated with reflux for 6 h (monitored by TLC), the reaction mixture was cooled and diluted with cold water, and the formed precipitated was filtered off. Beige powder (EtOH), mp = 236–238 °C. Yield 65%. IR (KBr) spectrum, ν, cm^{-1}: 3441 (NH), 2225 (C≡N) and 1647, 1668 (2C=O, amide). ^1H NMR (DMSO-d_6), δ (ppm): 1.14 (t, 3H, ^3J = 12.68 Hz, $CH_2C\underline{H}_3$), 1.25–1.80 (m, 11H, $H_{cyclohexyl}$), 4.31 (q, 2H, ^3J = 11.84 Hz, $C\underline{H}_2CH_3$), 7.33 (d, 2H, J = 8.24 Hz, Ar–H), 7.51 (d, 2H, J = 8.24 Hz, Ar–H), 13.22 (s, 1H, NH exchange with D_2O). ^{13}C NMR (DMSO-d_6), δ (ppm): 25.00, 25.82, 31.68, 54.10 (*O*–CH_2), 101.5, 105.2, 115.4 (C≡N), 128.4, 128.7, 129.5, 133.8, 135.7, 153.7, 155.8, 156.9, 160.1 and 160.5. Anal. calcd for $C_{22}H_{21}ClN_4O_3$ (424.88): C, 62.19; H, 4.98; N, 13.19. Found: C, 62.22; H, 4.97; N, 13.18.

2.1.9. 5-(4-Chlorophenyl)-8-cyclohexyl-4,7-dioxo-3,4,7,8-tetrahydropyrido[2,3-*d*]pyrimidine-6-carbonitrile (9). A mixture of *N*-cyclohexyl pyridone **2** (0.01 mol) and formamide (25 mL) was refluxed for 4 h (monitored by TLC), the reaction mixture was cooled, and the formed precipitate was filtered off and dried. Pale yellow (EtOH), mp = 280–282 °C. Yield 45%. IR (KBr), ν, cm^{-1}: 3390 (NH), 2222 (C≡N) and 1681 (br, 2C=O, amide). ^1H NMR (DMSO-d_6), δ (ppm): 1.23–1.87 (m, 11H, $H_{cyclohexyl}$), 7.35 (m, 4H, Ar–H), 7.95 (s, 1H, Ar–H), 13.22 (s, 1H, NH exchange with D_2O). Anal. calcd for $C_{20}H_{17}ClN_4O_2$ (380.83): C, 63.08; H, 4.50; N, 14.71. Found: C, 63.04; H, 4.51; N, 14.73.

2.1.10. 5-(4-Chlorophenyl)-8-cyclohexyl-4,7-dioxo-2-thioxo-1,2,3,4,7,8-hexahydropyrido[2,3-*d*]pyrimidine-6-carbonitrile (10). A mixture of *N*-cyclohexyl pyridone **2** (0.01 mol) and carbon disulfide (0.011 mol) in abs. EtOH (20 mL) was refluxed in the presence KOH (0.012 mol.) for 10 h. The completion of the reaction was monitored by TLC. The reaction mixture was cooled to room temperature, then poured into crushed ice then neutralized with HCl, and the formed precipitate was filtered off and dried. Dark brown powder (EtOH), mp = 310–312 °C. Yield 85%. IR (KBr) spectrum, ν, cm^{-1}: 3326 (2NH), 2208 (C≡N) and 1670, 1643 (2C=O, amide) and 1323 (C=S). ^1H NMR (DMSO-d_6) δ (ppm): 1.08–1.66 (m, 11H, $H_{cyclohexyl}$), 7.25 (d, 2H, J = 8.32 Hz, Ar–H), 7.38 (d, 2H, J = 8.20 Hz, Ar–H), 11.20, 12.60 (s, 2H, 2NH, exchange with D_2O). ^{13}C NMR (DMSO-d_6), δ (ppm): 23.48, 24.14, 25.06, 32.10, 107.7, 116.7 (C≡N), 128.2, 129.3, 130.3, 130.7, 131.5, 132.7, 133.1, 134.8, 148.5, 161.5. Anal. calcd for $C_{20}H_{17}ClN_4O_2S$ (412.89): C, 58.18; H, 4.15; N, 13.57. Found: C, 58.09; H, 4.17; N, 13.52.

2.1.11. 5-(4-Chlorophenyl)-8-cyclohexyl-4,7-dioxo-3,4,7,8-tetrahydropyrido[2,3-*d*][1,2,3]triazine-6-carbonitrile (11). To a suspended solution of *N*-cyclohexyl pyridone **2** (0.01 mol) in conc. HCl (30 mL) at 0–5 °C, a solution of $NaNO_2$ (3.0 g in 10 mL H_2O) was added over 20 min. After 2 h of stirring at r.t., the formed precipitate was collected by filtration, then washed with ice-cold water and dried. Orange powder (EtOH), mp = 162–164 °C. Yield 97%. IR (KBr) spectrum, ν, cm^{-1}: 3233 (NH), 2223 (C≡N), 1681 (2C=O, amide) and 1549 (N=N). ^1H NMR (DMSO-d_6), δ (ppm): 1.04–1.58 (m, 11H, $H_{cyclohexyl}$) 7.18 (d, 2H, J = 8.32 Hz, Ar–H), 7.29 (d, 2H, J = 8.32 Hz, Ar–H), 11.81 (s, 1H, NH exchange with D_2O). Anal. calcd for $C_{19}H_{16}ClN_5O_2$ (381.82): C, 59.77; H, 4.22; N, 18.34. Found: C, 59.78; H, 4.25; N, 18.35.

2.2. Biology

2.2.1. Cytotoxicity. Both breast cancer (MCF-7) and liver cancer (HepG2) and normal (MCF-10A) cells were purchased from the National Research Institute, Egypt, and maintained in RPMI-1640 medium L-glutamine (Lonza Verviers SPRL, Belgium, cat#12-604F). All cells were incubated at 37 °C in a 5% carbon dioxide atmosphere (NuAire). Cells were plated at a density of 5×10^4 cells in triplicates in 96 wells. On the second day, cells were treated with the compounds with concentrations of (0.01, 0.1, 1, 10, and 100 μM). Cell viability was assessed using the MTT assay.[22,23]

2.2.2. PIM-1 kinase inhibitory assay. Compounds **4**, **6**, **10**, **11**, and staurosporine were evaluated for the PIM-1 kinase inhibition using "HTScan® PIM-1 Kinase Assay Kit #7573". They were dissolved in DMSO (0.1%), and four serial concentrations were prepared following Abdelaziz *et al.* 2018 (ref. 24) and the manufacturer's instructions.[25]

2.2.3. Investigation of apoptosis

2.2.3.1. Annexin V/PI staining and cell cycle analysis. MCF-7 cells were seeded into 6-well culture plates (3–5 × 10^5 cells per well) and incubated overnight. Cells were treated with compound **4** at their IC_{50} values for 48 h. Next, media supernatants and cells were collected and rinsed with ice-cold PBS. Then, cells were suspended the cells in 100 μL of annexin binding buffer solution "25 mM $CaCl_2$, 1.4 M NaCl, and 0.1 M Hepes/NaOH, pH 7.4" and incubated with "annexin V-FITC solution (1 : 100) and propidium iodide (PI)" at a concentration equals 10 μg mL^{-1} in the dark for 30 min. Stained cells were then acquired by BD FACSCalibur™ Flow Cytometer.[26–28]

2.2.3.2. Real time-polymerase chain reaction for the selected genes. Gene expression of Bcl-2, the anti-apoptotic gene, and the pro-apoptotic genes P53, Bax, and caspases-3,8,9 were examined to delve deeper into the apoptotic pathway. MCF-7 cells were treated with compound **4** at their IC_{50} values for 48 h. After treatment, the RT-PCR reaction was carried out following routine work. Then, the C_t values were collected to calculate the relative genes' expression in all samples by normalization to the β-actin housekeeping gene.[26,29]

2.2.4. Molecular docking. The protein structure of PIM-1 kinase (PDB 2OBJ) was obtained from the protein data bank and was optimized by adjusting the amino acids, and ligand structures were built, optimized, and energetically favored using Maestro. A molecular docking study was carried out using AutoDock Vina software following routine work,[30] and finally, docking with binding activities in terms of binding energies and ligand–receptor interactions. Chimera was used to analyze the binding disposition and interactive analysis.

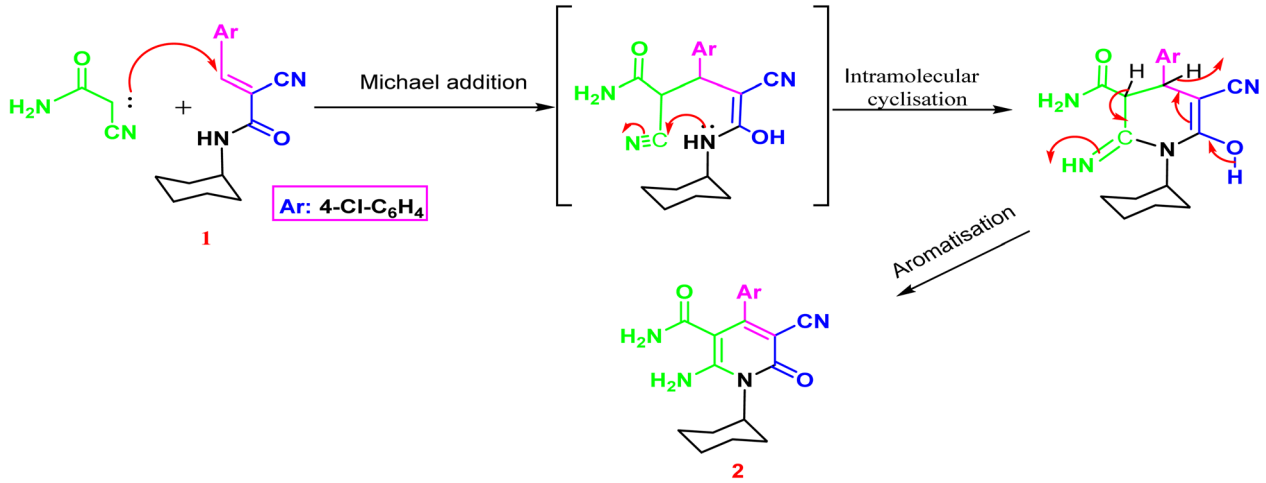

Scheme 1 The plausible mechanism for the formation of 1,6-dihydropyridine-3-carboxamide **2**.

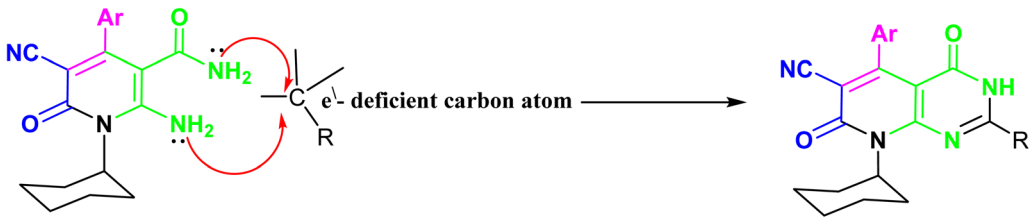

Fig. 3 The plausible cyclization of pyrimidine nucleus.

3 Results and discussion

3.1. Chemistry

The synthesis of the target *o*-aminonicotinoamide **2** was outlined in (Scheme 1) *via* Michael type addition of cyanoacetamide to 2-cyano-*N*-cyclohexyl acrylamide (**1**) followed by intramolecular cyclization in the presence of piperidine as a mild catalytic base. The reaction smoothly proceeded in ethanol, and the product was obtained in high yield (91%).

The characteristic IR bands of **2** show the presence of stretching bands at 3325, 3300, 2210, 1665 and 1650 cm^{-1} for $2NH_2$, CN, and 2C=O, which evidence the formation of the structure. The ^1H NMR signals confirm its formation *via* the presence of cyclohexyl protons as multiplet at 0.72–1.46 ppm, and the two amino groups appeared as two main singlets at δ_H 6.96 and 11.45 ppm, which exchange with D_2O. Furthermore, the aromatic protons split into two doublets at 7.29 and 7.51 ppm with a coupling constant (J = 8.80 Hz). The nicotinamide **2** contains *o*-amino-amide functions that enable such compounds to act as trapping for an electron-deficient carbon atom, resulting in cyclization and formation of a new annulated pyrimidine nucleus Fig. 3.

The acylation of nicotinamide **2** with acid chloride, namely, (benzoyl chloride, 2,4-dichloro benzoyl chloride, furoyl chloride, chloroacetyl chloride) and ester (*e.g.* diethyl oxalate), triethylorthoformate and formamide or thio acylation with carbon disulfide afforded the corresponding pyrido[2,3-*d*] pyrimidine **3–10** according to (Schemes 2 and 3). The structure of the desired compound is agreed with their spectral analysis. For example, the IR confirms the disappearance of the primary NH_2 groups and the presence of secondary NH between 3441 and 3271. The ^1H NMR spectra are another evidence for the formation of the target pyrimidines.

Compound **3** shows the presence of phenyl group in its ^1H NMR spectrum as doublet, multiplet, and triplet at 7.32, 7.38, and 7.50 ppm, respectively. Cyclization of 2-amino-1,6-dihydropyridine-3-carboxamide **2** with chloroacetyl chloride yielded pyridopyrimidinone **6**. The IR spectrum revealed the absorption band of NH at 3429 cm^{-1} and C≡N function at 2215 cm^{-1}. While the two carbonyl amide groups appeared as broad band at 1665 cm^{-1}. The ^1H NMR spectrum showed a singlet signal at 4.73 ppm assigned for the two protons of CH_2 and a singlet signal at δ = 11.88 ppm for NH proton. On the other hand, compound **2** underwent refluxing with diethyl oxalate in DMF to afford the pyridopyrimidine ester derivative **7**. Compound **7** shows the presence of ethyl ester group *via* the presence of C=O ester in its IR at 1718 cm^{-1} and ethyl group of ester as triplet and quartet at 1.18 and 4.37 ppm in its ^1H NMR, in addition to NH proton at 8.10 ppm. Also, the structures of **8**, **9**, and **10** were confirmed by the usual spectroscopic techniques

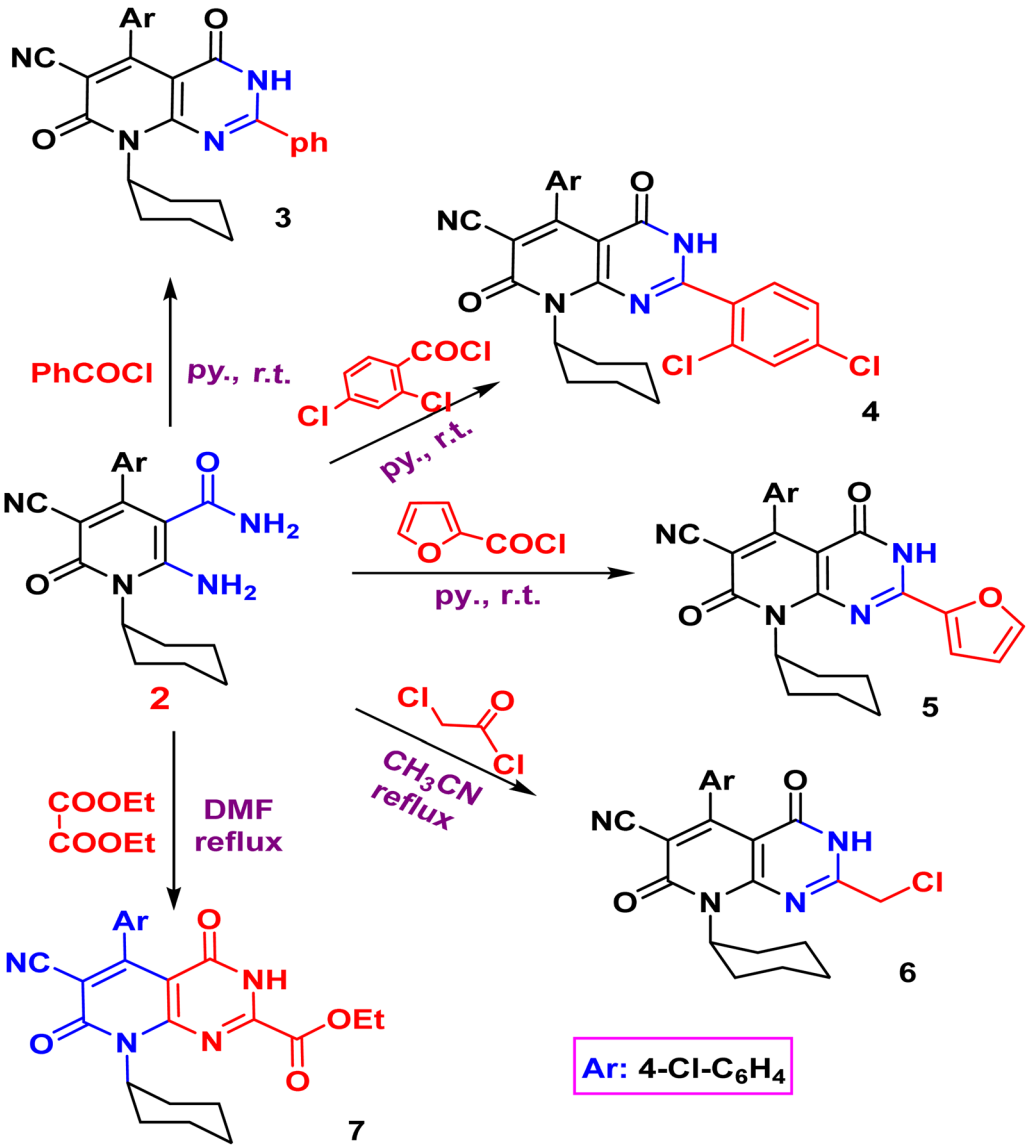

Scheme 2 Synthesis of 2-arylpyrido[2,3-*d*]pyrimidines **3–7**.

and elemental analysis. The IR spectra of compound **8** displayed a lack of the significant two amino group bands and the presence of a strong stretching NH group at 3441 cm^{-1}. Additionally, the ^1H NMR spectra for the same compound **8** assigned specific triplet and quartet signals for ethoxy protons at δ 1.14 and 4.31 ppm, respectively, as well as, NH proton at δ 13.22 as a singlet. The IR spectrum of compound **9** showed characteristic absorption bands at 3390 cm^{-1} for (NH). Another evidence for pyrimidine ring formation is the significant singlet signal corresponding to (CH) at 7.95 ppm.

Finally, the pyrido[2,3-*d*]triazine **11** was obtained in high yield (97%) *via* diazotization of nicotinamide **2** with nitrous acid. The expected structure was elucidated through the IR spectrum, in which a significant band for (NH), (2C=O), and (N=N, triazine) stretched at ν 3233, 1681, and 1549 cm^{-1}, respectively. Moreover, the ^1H NMR spectrum displayed significant signals at δ 1.04–1.58 ppm for cyclohexyl protons, and the aromatic protons appeared as doublets at 7.18 and 7.29 ppm, in addition to the characteristic singlet at 11.81 ppm for NH group.

3.2. Biology

3.2.1. Cytotoxicity. The MTT test evaluated the synthesized compounds for their cytotoxicity against MCF-7 and HepG2 cells. As seen in Table 1, compounds **4**, **6**, **9**, **10**, and **11** exhibited potent cytotoxicity against MCF-7 cells with IC_{50} values range (0.57–3.15 μM) compared to staurosporine (IC_{50} = 6.76 μM). Additionally, compounds **2**, **5**, **7**, and **8** exhibited promising cytotoxicity with IC_{50} values range (16.9–29.6 μM). At the same time, other compounds were non-toxic with higher IC_{50} values.

Against HepG2 cells, compounds **4**, **6**, **9**, **10**, and **11** exhibited potent cytotoxicity against HepG2 with IC_{50} values range (0.99–

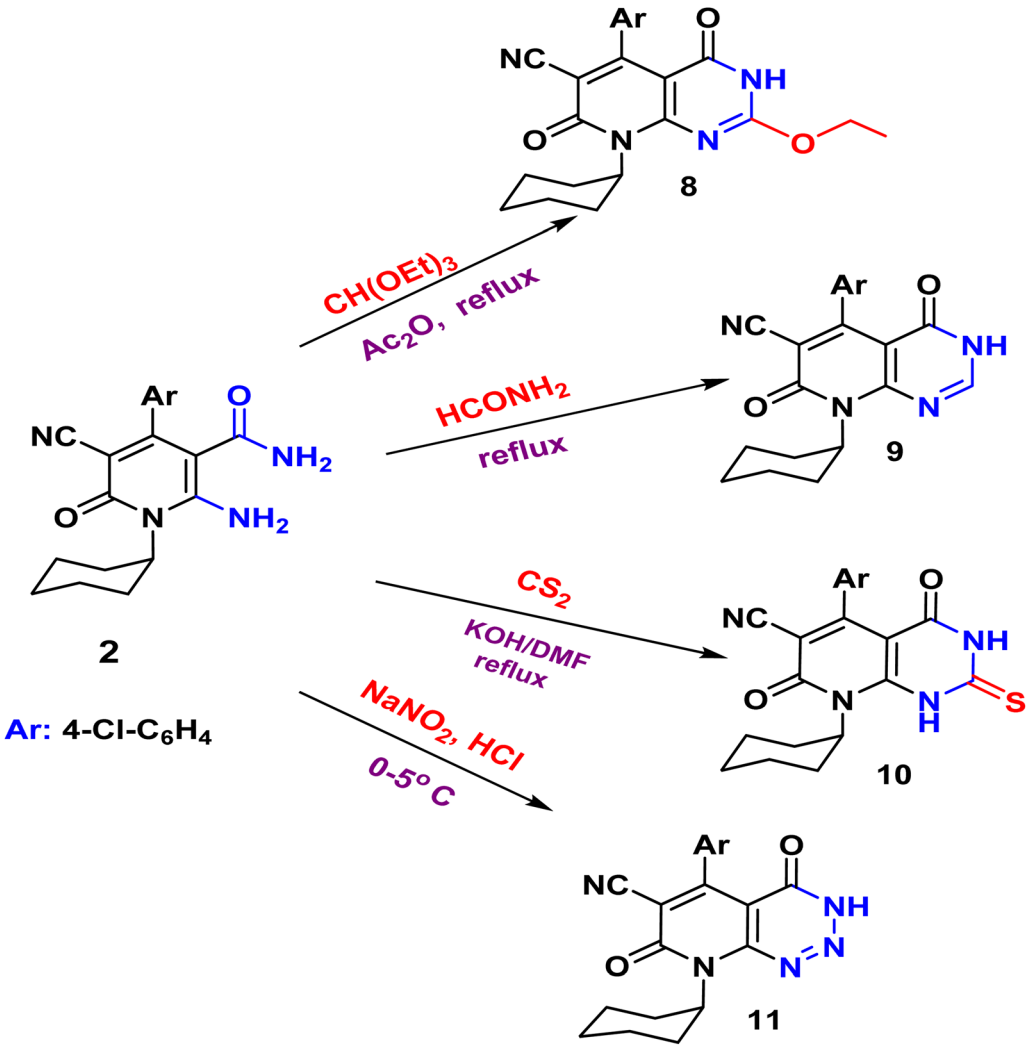

Scheme 3 Synthesis of pyridopyrimidines and triazine (**8–10** and **11**).

Table 1 Cytotoxic IC_{50} values of the tested compounds against MCF-7, HepG2, and MCF-10A cell lines using the MTT assay[a]

	$IC_{50} \pm SD$ [μM]		
Compounds no.	MCF-7	HepG2	MCF-10A
2	16.9 ± 0.45	15.6 ± 0.69	NT
3	≥50	1.17 ± 0.24	NT
4	0.57 ± 0.14	1.13 ± 0.19	47.6 ± 3.1
5	11.2 ± 0.54	13.4 ± 0.27	NT
6	1.29 ± 0.23	2.1 ± 0.24	43.5 ± 2.9
7	29.6 ± 0.8	≥50	NT
8	9.6 ± 0.24	8.1 ± 0.24	NT
9	3.15 ± 0.14	4.6 ± 0.34	NT
10	1.4 ± 0.24	1.79 ± 0.14	≥50
11	1.31 ± 0.28	0.99 ± 0.17	≥50
Staurosporine	6.76 ± 0.51	5.07 ± 0.36	NT

[a] Values are expressed as mean ± SD of three independent triplets ($n = 3$). NT: non-tested. Staurosporine is a potent anticancer agent as a potent PIM-1 kinase inhibitor.[31]

4.16 μM) compared to staurosporine (IC_{50} = 5.07 μM). Additionally, compounds **2**, **5**, and **8** exhibited promising cytotoxicity with IC_{50} values range (8.1–15.6 μM). At the same time, other compounds were non-toxic with higher IC_{50} values.

As shown in Fig. 4 for the dose–response curve of cell viability *versus* the tested concentration of compound **4** against MCF-7, HepG2 and MCF-10A cells. It caused the highest percentage of cell viability of cancer cells at the highest concentration, while it caused the lowest viability of normal cells; this highlighted the selectivity profile of compound **4**. Furthermore, compounds **4**, **6**, **10**, and **11** were worthy of investigation for their cytotoxicity against normal MCF-10A cells, and they were non-toxic with much higher IC_{50} values.

Comparing the structure and the cytotoxicity of tested compounds, a valid SAR model can be generated as summarized in Fig. 5. Incorporating hydrophilic, aromatic, hydrogen bond donors and acceptors caused an increase in cytotoxicity, particularly in compounds **4**, **6**, **10** and **11**.

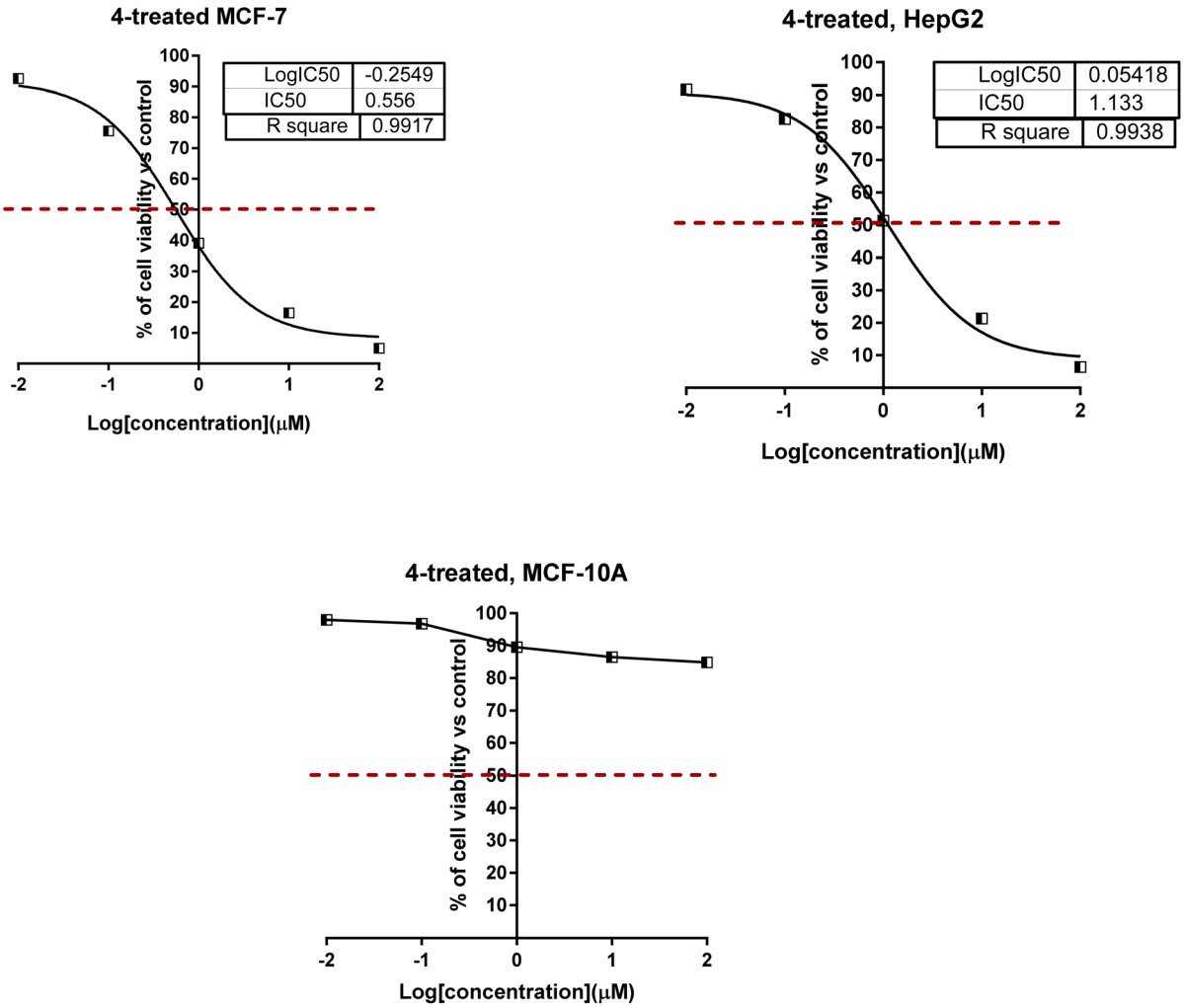

Fig. 4 Dose–response nonlinear regression curve fitting the percentage of cell viability *vs.* log[con. μM], *R* square ≈ 1 using the GraphPad prism.

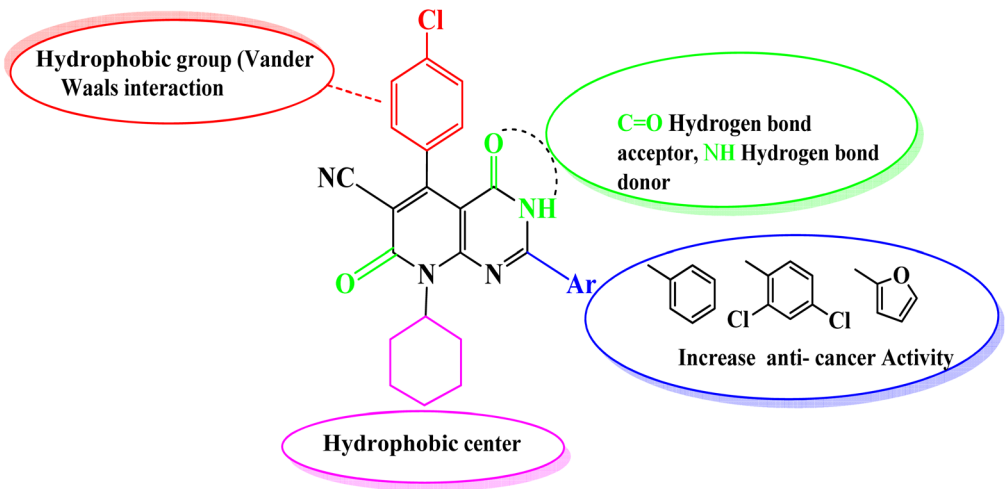

Fig. 5 Structure–activity relationship (SAR) model for the activity of the designed derivatives. Substituents anchored on the main scaffold with cytotoxic activities.

Table 2 IC_{50} values of PIM-1 kinase inhibition of the most cytotoxic compounds

Compound	% of PIM-1 inhibition	$IC_{50} \pm SD^a$ (nM)
4	97.8 ± 1.8	11.4 ± 0.13
6	89.6 ± 2.1	34.6 ± 0.18
10	94.6 ± 2.1	17.2 ± 0.20
11	92.1 ± 1.9	21.4 ± 0.24
Staurosporine	95.6 ± 2.4	16.7 ± 0.32
Pyrido[4,3-*d*]pyrimidine-derivative inhibitor (SKI-O-068)[32]	—	123 ± 14

[a] Values are expressed as an average of three independent replicates. "IC_{50} values were calculated using sigmoidal non-linear regression curve fit of percentage inhibition against five concentrations of each compound".

3.2.2. PIM-1 kinase inhibitory assay. To identify their molecular targets, compounds **4**, **6**, **10**, and **11** were evaluated against the PIM-1 inhibitory activities. These compounds had the highest cytotoxic activity against MCF-7 cells. As seen in Table 2, the tested compounds showed promising PIM-1 kinase inhibition activity; interestingly, compounds **4** and **10** had IC_{50} values of 11.4 and 17.2 nM, respectively, with inhibition of 97.8% and 94.6%, compared to staurosporine (IC_{50} = 16.7 nM, with 95.6% inhibition). Additionally, compounds **6** and **11** exhibited promising PIM-1 inhibition with IC_{50} values of 34.6 and 21.4 nM with inhibition activity of 89.6% and 92.1%, respectively. As a result, compound **4** was studied for its ability to inhibit PIM-1 kinase and induce apoptotic cell death in MCF-7 cells. Additionally, the tested compounds exhibited potent PIM-1 kinase inhibition more than a previously reported pyrido[4,3-*d*]pyrimidine-derivative with IC_{50} of 123 nM that was deposited in a crystal structure of PIM-1 kinase protein.[32]

3.2.3. Apoptotic investigation

3.2.3.1. Annexin V/PI staining with cell cycle analysis. The apoptotic activity of compound **4** (IC_{50} = 0.57 μM, 48 h) was determined by using flow cytometric analysis of annexin V/PI staining to investigate apoptotic cell death in both untreated and treated MCF-7 cells. Fig. 6 (top panel) showed compound **4**

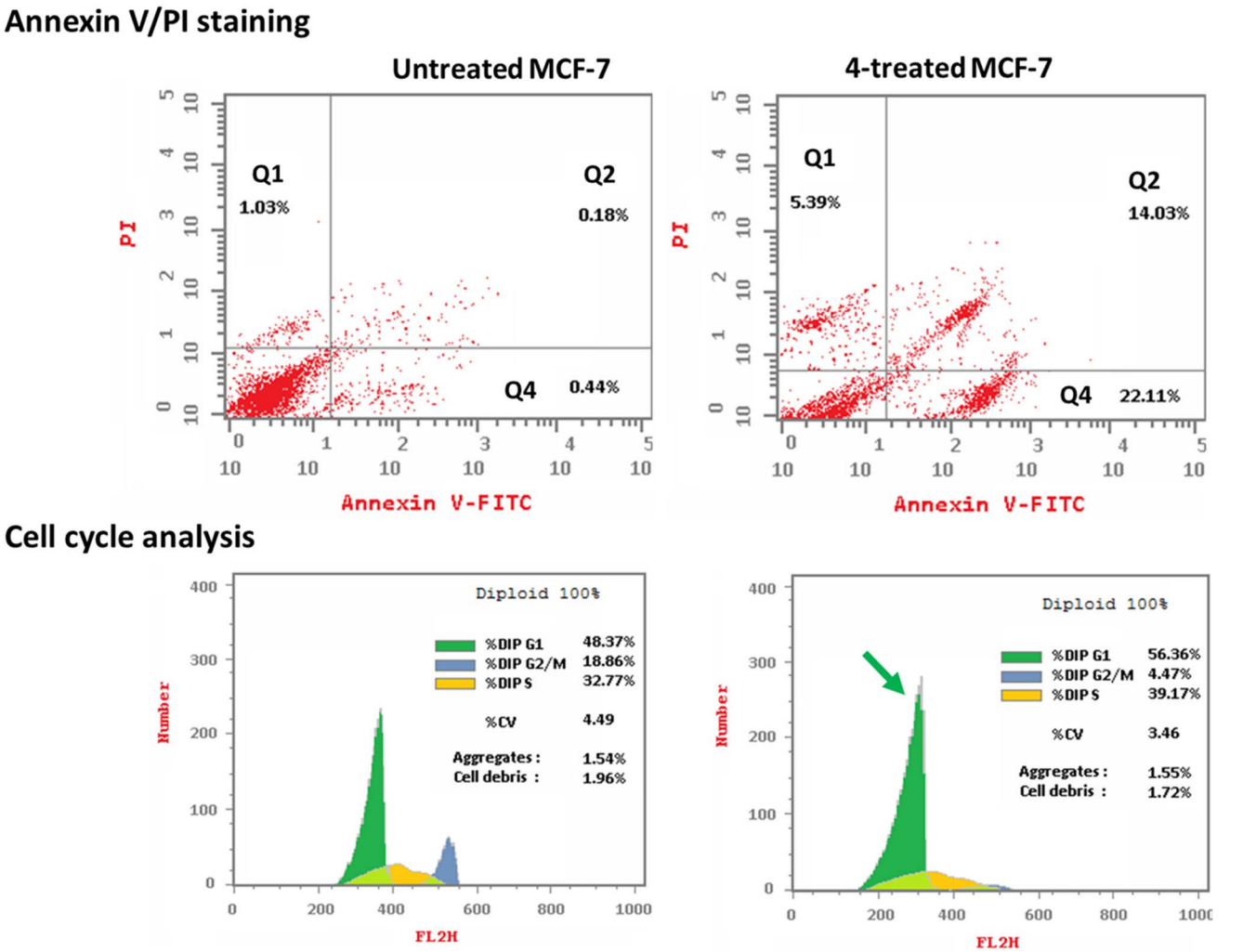

Fig. 6 Cryptographs of annexin-V/propidium iodide staining of untreated and **4**-treated MCF-7 cells with (IC_{50} = 0.57 μM, 48 h). Percentage of cell population at each cell cycle "G1, S, and G2/M" using DNA content-flow cytometry aided cell cycle analysis.

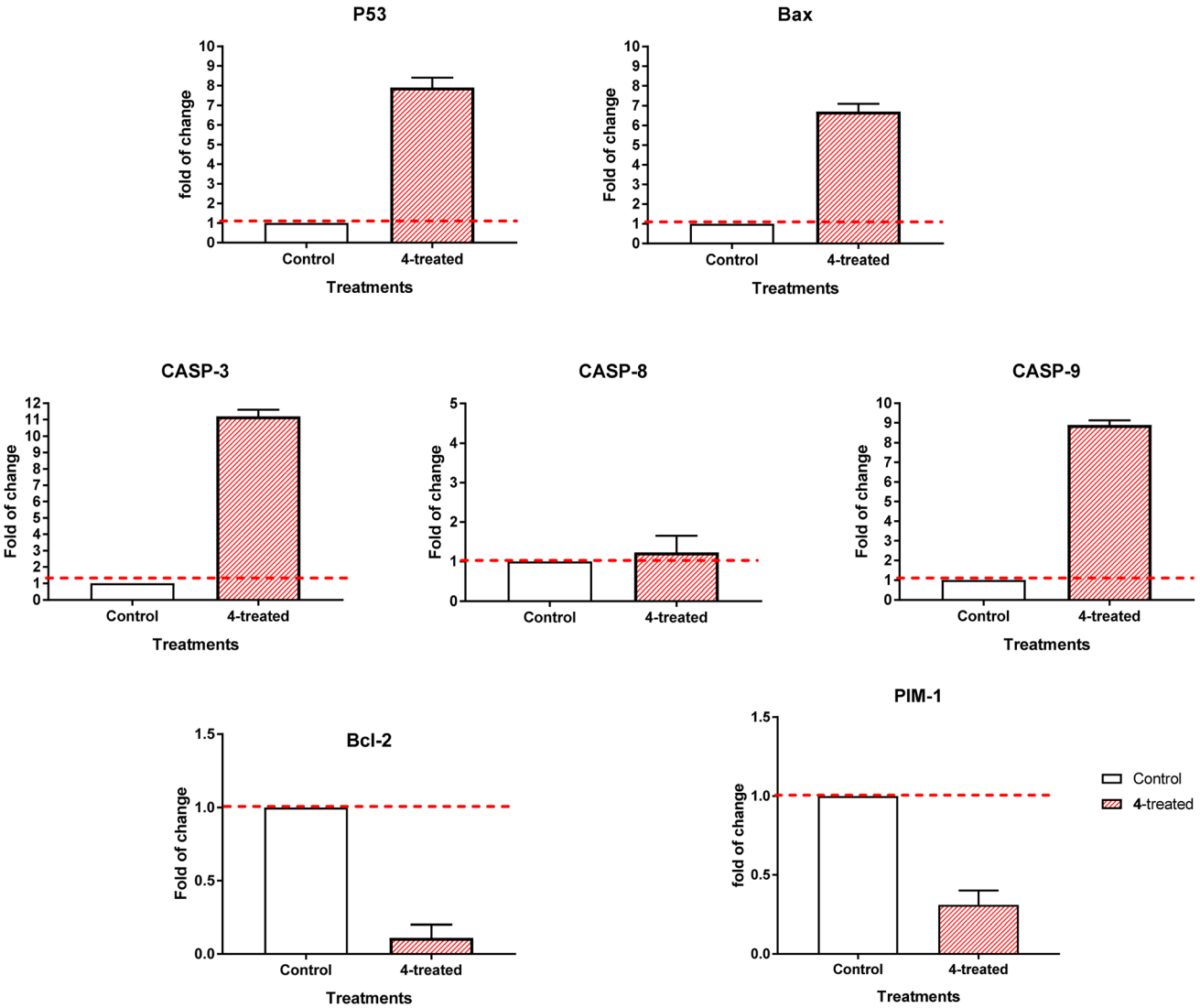

Fig. 7 Quantitative RT-PCR results analysis of the apoptosis-related genes; P53, Bax, caspases-3,8,9, Bcl-2 and PIM-1 kinase, respectively in MCF-7 cells treated with compound **4** with (IC_{50} = 0.57 μM, 48 h). The data illustrated is the average of 3 independent experimental runs (mean ± SD). The red dashed line represents the fold change of control = 1.

dramatically induced apoptotic cell death in MCF-7 cells, increasing the death rate by 58.3-fold; it induced total apoptosis by 36.14% (14.03% for late apoptosis, 22.11% for early apoptosis) compared to the untreated control group (0.62%).

The cell population in each cell phase after cytotoxic agent treatment was then determined by DNA flow cytometry. As seen in Fig. 6 (bottom panel), compound **4** treatment significantly increased the cell population at the G1-phase by 56.36% compared to control 48.37%, while cells in the G2/M-phase were decreased (4.47% compared to 18.86%). Compound **4** caused cell death in MCF-7 cells, stopping their growth in the G1 phase.

3.2.3.2. RT-PCR. By comparing the RT-PCR levels of the apoptosis-mediated genes P53, Bax, caspase-3,8,9, and Bcl-2 in both the untreated and treated MCF-7 cells, we could confirm that compound **4** caused cell death in these cells. As seen in Fig. 7, compound **4** upregulated caspase-3,8,9 levels by 11.2, 1.23, and 8.9-fold, Bax by 6.7-fold, and P53 by 7.9-fold, while it downregulated the Bcl-2 expression by 0.11-fold and inhibited the PIM-1 expression by 0.31-fold. Consequently, our results demonstrated that compound **4** treatment caused cell death by apoptosis *via* an intrinsic mechanism through inhibition of PIM-1 kinase.

The ubiquitous PIM kinases regulate various biological events, including cell proliferation, cell differentiation, and cell death. When expressed in ways that worsen cancer, these genes, which function as weak oncogenes, cause a variety of human cancers. Thus, PIM kinase inhibition may be a valuable therapeutic target for cancer.[33] Among heterocycles, pyridine derivatives showed cell cycle stop and apoptosis induction capabilities and could be considered a potential PIM-1 kinase inhibitor. These compounds could be explored as potential treatments for breast cancer.[34] Compound **4** as concluded from

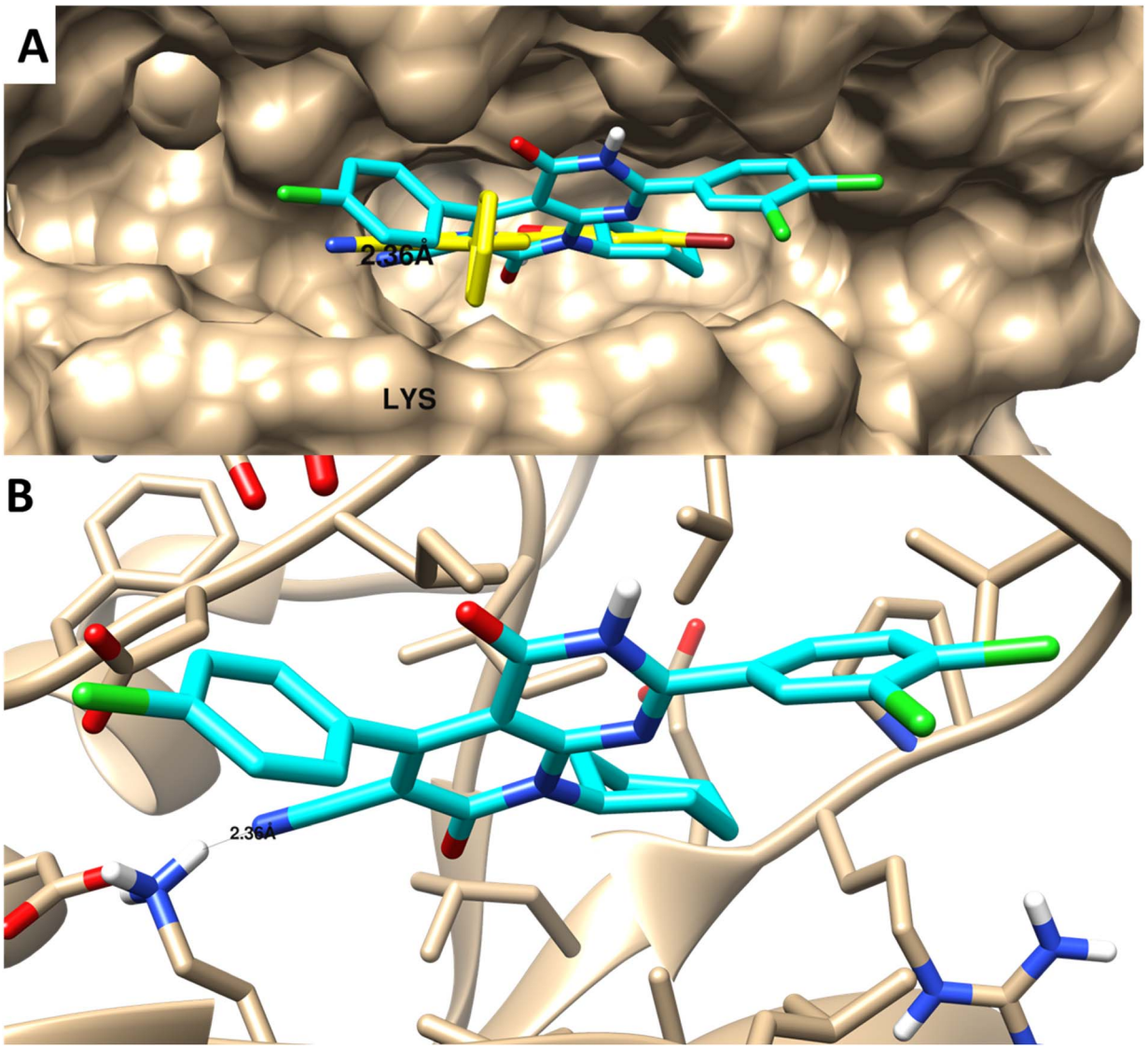

Fig. 8 Molecular docking of **4** towards PIM-1 protein (PDB 2OBJ). (A) Surface disposition of the co-crystallized ligand (yellow-colored) and the docked compound (cyan-colored) and (B) interactive view of the compound with the highlighted key amino acids. 3D images were generated by Chimera-UCSF software.

Table 3 Molecular properties and ADME pharmacokinetics of the promising compounds[a]

	Molsoft				Molinspiration 2018.10						SwissADME
#	HBA	HBD	Solubility (mg L^{-1})	Drug score	MWt (D)	MV ($Å^3$)	PSA ($Å^2$)	Log *p*	BBB score	$n_{violations}$	Drug likeness (Lipinski Pfizer filter)
4	4	1	1.25	0.84	490	507.4	65.99	5.0	3.84	0	Yes
6	4	1	134.68	0.12	394.12	433.08	66.27	3.23	3.71	0	Yes
10	4	2	91.36	0.0	378.12	430.63	67.20	3.12	2.74	0	Yes
11	5	1	230.53	−0.22	347.14	393.24	81.13	2.76	3.12	0	Yes

[a] "Mwt: molecular weight, MV: molecular volume, PAS: polar surface area, log *p*: log *p*: octanol–water partition coefficient, nrotb: number of rotatable bonds, $n_{violations}$: number of violations, HBA: hydrogen bond acceptor, HBD: hydrogen bond donor, drug-likeness score, compounds having negative or zero value should not be considered as drug-like". Drug likeness (Lipinski Pfizer filter)/"yes, drug-like" MW ≤ 500, log *p* ≤ 4.25, HBA ≤ 10 and HBD ≤ 5".

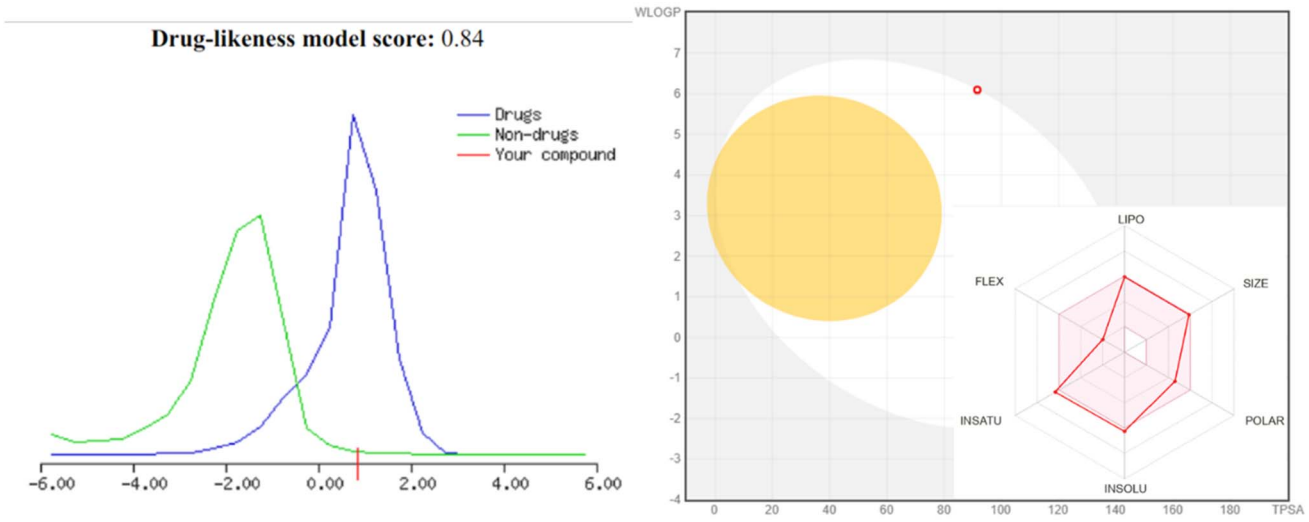

Fig. 9 Drug likeness score of compound **4** using MolSoft "the green color means non-drug-like behavior, and those that fall under blue color area are considered as drug-like. Those compounds having negative or zero value should not be considered as a drug like". BOILED-Egg model for compound **4** using SwissADME molecules projected to passively cross the blood–brain barrier (BBB) is positioned in the yolk of the BOILED-Egg, while those predicted to be passively absorbed by the gastrointestinal tract (GI) are in the white of the egg.

this study; it may solve some problems of pyridine and pyridopyrimidine containing anticancer molecules by having more potent and target-oriented chemotherapeutics (apoptosis-induction) with selective profile against normal cells.

3.3. *In silico* studies

3.3.1. Molecular docking. As seen in Fig. 8, compound **4** was docked inside the PIM-1 binding site, having the same binding mode as the co-crystallized ligand. Docking results exhibited that the compound was properly docked inside the PIM-1 active site with a binding energy of -20.84 kcal mol^{-1}, and it formed one stable hydrogen bond interaction through the cyano-group with Lys 67 amino acid with a bond length of 2.36 Å. So, the molecular docking study validated the experimental enzyme target activity of PIM-1 kinase inhibition, which seems to be the effective target for apoptosis-mediated cell death.

3.3.2. Physicochemical and pharmacokinetic properties. The promising compounds **4**, **6**, **10**, and **11** were investigated for their physicochemical and drug-likeness properties. As seen in Table 3 and Fig. 9, they exhibited promising values following Lipinski's rule of five of "molecular weight, number of rotatable bonds, H-bond donor, and acceptors along with a number of violations".

4 Conclusion and recommendations

New series of pyrido[2,3-*d*]pyrimidine was described. Nicotinamide **2** was synthesized *via* cyclization of *N*-cyclohexyl derivative with cyanoacetamide. The *o*-aminonicotinonitrile **2** was subjected to acylation or thioacylation process followed by intramolecular heterocyclization to afford the desired pyrido[2,3-*d*]pyrimidine (**3–11**). Among these derivatives, compound **4** exhibited remarkable cytotoxic activities against MCF-7 and HepG2 cells with IC_{50} values of 0.57 μM and 1.13 μM, respectively. Interestingly, compound **4** had potent PIM-1 kinase inhibition with IC_{50} values of 11.4 nM, respectively, with inhibition of 97.8% compared to staurosporine (IC_{50} = 16.7 nM, with 95.6% inhibition). Moreover, compound **4** significantly induced apoptosis in MCF-7 cells by 58.29-fold by having 36.14% total apoptosis in treated cells compared to 0.62% for control. Moreover, arresting the cell cycle at the G1-phase. Accordingly, compound **4** was validated as a promising PIM-1 targeted chemotherapeutic agent to treat breast cancer. Accordingly, the anticancer activity of compound **4** will be further validated in the future using *in vivo* study as a real animal model.

Author contributions

E. S. Tantawy, S. M. Mohammed, H. A. Morsy, H. A. El-Sayed, and A. H. Moustafa synthesized the entire series of derivatives with the characterization of structure elucidation, while M. S. Nafie initiated the idea and design of the biology part by carrying out *in vitro* cytotoxic screening, flow cytometry, RT-PCR analysis, and *in silico* studies with the linguistic revision and manuscript finalizing. All authors contributed to data analysis and manuscript writing original draft in their corresponding parts. All authors validated it in the final submitted form.

Conflicts of interest

The authors declare no conflict of interest.

References

1 T. Al-Warhi, A. A. Al-Karmalawy, A. A. Elmaaty, M. A. Alshubramy, M. Abdel-Motaal, T. A. Majrashi, M. Asem, A. Nabil, W. M. Eldehna and M. Sharaky,

Biological evaluation, docking studies, and *in silico* ADME prediction of some pyrimidine and pyridine derivatives as potential EGFR(WT) and EGFR(T790M) inhibitors, *J. Enzyme Inhib. Med. Chem.*, 2023, **38**, 176–191, DOI: **10.1080/14756366.2022.2135512**.

2 W. Cao, H.-D. Chen, Y.-W. Yu, N. Li and W.-Q. Chen, Changing profiles of cancer burden worldwide and in China: a secondary analysis of the global cancer statistics 2020, *China Med. J.*, 2021, **134**, 783–791, DOI: **10.1097/CM9.0000000000001474**.

3 E. A. Madbouly, E.-S. M. Lashine, A. A. Al-Karmalawy, M. M. Sebaiy, H. Pratsinis, D. Kletsas and K. Metwally, Design and synthesis of novel quinazolinone–chalcone hybrids as potential apoptotic candidates targeting caspase-3 and PARP-1: *in vitro*, molecular docking, and SAR studies, *New J. Chem.*, 2022, **46**, 22013–22029, DOI: **10.1039/d2nj04053k**.

4 W. M. Eldehna, R. M. Maklad, H. Almahli, T. Al-Warhi, E. B. Elkaeed, M. A. S. Abourehab, H. A. Abdel-Aziz and A. M. El Kerdawy, Identification of 3-(piperazinylmethyl) benzofuran derivatives as novel type II CDK2 inhibitors: design, synthesis, biological evaluation, and *in silico* insights, *J. Enzyme Inhib. Med. Chem.*, 2022, **37**, 1227–1240, DOI: **10.1080/14756366.2022.2062337**.

5 T. Al-Warhi, M. M. Elbadawi, A. Bonardi, A. Nocentini, A. A. Al-Karmalawy, N. Aljaeed, O. J. Alotaibi, H. A. Abdel-Aziz, C. T. Supuran and W. M. Eldehna, Design and synthesis of benzothiazole-based SLC-0111 analogues as new inhibitors for the cancer-associated carbonic anhydrase isoforms IX and XII, *J. Enzyme Inhib. Med. Chem.*, 2022, **37**, 2635–2643, DOI: **10.1080/14756366.2022.2124409**.

6 A. Sabt, W. M. Eldehna, T. Al-Warhi, O. J. Alotaibi, M. M. Elaasser, H. Suliman and H. A. Abdel-Aziz, Discovery of 3,6-disubstituted pyridazines as a novel class of anticancer agents targeting cyclin-dependent kinase 2: synthesis, biological evaluation and *in silico* insights, *J. Enzyme Inhib. Med. Chem.*, 2020, **35**, 1616–1630, DOI: **10.1080/14756366.2020.1806259**.

7 L. Akl, A. A. Abd El-Hafeez, T. M. Ibrahim, R. Salem, H. M. M. Marzouk, R. A. El-Domany, P. Ghosh, W. M. Eldehna and S. M. Abou-Seri, Identification of novel piperazine-tethered phthalazines as selective CDK1 inhibitors endowed with *in vitro* anticancer activity toward the pancreatic cancer, *Eur. J. Med. Chem.*, 2022, **243**, 114704, DOI: **10.1016/j.ejmech.2022.114704**.

8 L. K. Gediya and V. C. Njar, Promise and challenges in drug discovery and development of hybrid anticancer drugs, *Expert Opin. Drug Discovery*, 2009, **4**, 1099–1111, DOI: **10.1517/17460440903341705**.

9 B. Mansour, Y. A. Salem, K. M. Attallah, O. A. El-Kawy, I. T. Ibrahim and N. I. Abdel-Aziz, Cyanopyridinone- and Cyanopyridine-Based Cancer Cell Pim-1 Inhibitors: Design, Synthesis, Radiolabeling, Biodistribution, and Molecular Modeling Simulation, *ACS Omega*, 2023, **8**, 19351–19366, DOI: **10.1021/acsomega.2c08304**.

10 M. A. Waly, I. I. Elhawary and T. M. Elgogary, Utilization of nicotinonitrile-2-thiol in the synthesis of new thiepino[2,3-*b*]pyridine derivative as an *in vitro* novel antitumor potent, *Med. Chem. Res.*, 2012, **22**, 1674–1678, DOI: **10.1007/s00044-012-0161-4**.

11 A. Krauze, S. Grinberga, L. Krasnova, I. Adlere, E. Sokolova, I. Domracheva, I. Shestakova, Z. Andzans and G. Duburs, Thieno[2,3-b]pyridines—a new class of multidrug resistance (MDR) modulators, *Bioorg. Med. Chem.*, 2014, **22**, 5860–5870, DOI: **10.1016/j.bmc.2014.09.023**.

12 M. M. Ghorab, F. A. Ragab, H. I. Heiba, M. G. El-Gazzar and S. S. Zahran, Synthesis, anticancer and radiosensitizing evaluation of some novel sulfonamide derivatives, *Eur. J. Med. Chem.*, 2015, **92**, 682–692, DOI: **10.1016/j.ejmech.2015.01.036**.

13 A. Samadi, M. de la Fuente Revenga, C. Pérez, I. Iriepa, I. Moraleda, M. I. Rodríguez-Franco and J. Marco-Contelles, Synthesis, pharmacological assessment, and molecular modeling of 6-chloro-pyridonepezils: new dual AChE inhibitors as potential drugs for the treatment of Alzheimer's disease, *Eur. J. Med. Chem.*, 2013, **67**, 64–74, DOI: **10.1016/j.ejmech.2013.06.021**.

14 A. Samadi, M. Estrada, C. Pérez, M. I. Rodríguez-Franco, I. Iriepa, I. Moraleda, M. Chioua and J. Marco-Contelles, Pyridonepezils, new dual AChE inhibitors as potential drugs for the treatment of Alzheimer's disease: synthesis, biological assessment, and molecular modeling, *Eur. J. Med. Chem.*, 2012, **57**, 296–301, DOI: **10.1016/j.ejmech.2012.09.030**.

15 N. M. Khalifa, M. A. Al-Omar, H. M. Alkahtani and A. H. Bakheit, Kinase Inhibitors of Novel Pyridopyrimidinone Candidates: Synthesis and *In Vitro* Anticancer Properties, *J. Chem.*, 2019, **2019**, 1–10, DOI: **10.1155/2019/2635219**.

16 S. M. Mohammed, A. A. Masry, A. H. Moustafa, H. A. El-Sayed, E. M. Gad and H. A. Morsy, K_2CO_3-nanoparticles catalyzed the synthesis of 3-arylidine imidazo[1,2-c] pyrimidine candidates: Cytotoxic activity and docking study, *Synth. Commun.*, 2023, **53**, 1319–1332, DOI: **10.1080/00397911.2023.2220442**.

17 W. M. Eldehna, M. A. El Hassab, M. F. Abo-Ashour, T. Al-Warhi, M. M. Elaasser, N. A. Safwat, H. Suliman, M. F. Ahmed, S. T. Al-Rashood, H. A. Abdel-Aziz and R. El-Haggar, Development of isatin-thiazolo[3,2-*a*] benzimidazole hybrids as novel CDK2 inhibitors with potent *in vitro* apoptotic anti-proliferative activity: synthesis, biological and molecular dynamics investigations, *Bioorg. Chem.*, 2021, **110**, 104748, DOI: **10.1016/j.bioorg.2021.104748**.

18 A. T. A. Boraei, E. H. Eltamany, I. A. I. Ali, S. M. Gebriel and M. S. Nafie, Synthesis of new substituted pyridine derivatives as potent anti-liver cancer agents through apoptosis induction: *in vitro*, *in vivo*, and *in silico* integrated approaches, *Bioorg. Chem.*, 2021, **111**, 104877, DOI: **10.1016/j.bioorg.2021.104877**.

19 M. S. Nafie, A. M. Amer, A. K. Mohamed and E. S. Tantawy, Discovery of novel pyrazolo[3,4-b]pyridine scaffold-based

derivatives as potential PIM-1 kinase inhibitors in breast cancer MCF-7 cells, *Bioorg. Med. Chem.*, 2020, **28**, 115828, DOI: **10.1016/j.bmc.2020.115828**.

20 S. M. Shaban, E. H. Eltamany, A. T. A. Boraei, M. S. Nafie and E. M. Gad, Design and Synthesis of Novel Pyridine-Based Compounds as Potential PIM-1 Kinase Inhibitors, Apoptosis, and Autophagy Inducers Targeting MCF-7 Cell Lines: *In Vitro* and *In Vivo* Studies, *ACS Omega*, 2023, **8**, 46922–46933, DOI: **10.1021/acsomega.3c06700**.

21 A. Fahim, A. Farag, M. Shaaban and E. Ragab, Microwave Assisted Synthesis of Pyrazolo[1,5-*a*]pyrimidine, Triazolo [1,5-*a*]pyrimidine, Pyrimido[1,2-*a*]benzimdazole, Triazolo [5,1-*c*][1,2,4]triazine and Imidazo[2,1-*c*][1,2,4]triazine, Current Microwave, *Chemistry*, 2019, **5**, 111–119, DOI: **10.2174/2213335605666180425144009**.

22 T. Mosmann, Rapid colorimetric assay for cellular growth and survival: application to proliferation and cytotoxicity assays, *J. Immunol. Methods*, 1983, **65**, 55–63, DOI: **10.1016/0022-1759(83)90303-4**.

23 E. S. Tantawy, A. M. Amer, E. K. Mohamed, M. M. Abd Alla and M. S. Nafie, Synthesis, characterization of some pyrazine derivatives as anti-cancer agents: *in vitro* and *in silico* approaches, *J. Mol. Struct.*, 2020, **1210**, 128013, DOI: **10.1016/j.molstruc.2020.128013**.

24 M. E. Abdelaziz, M. M. M. El-Miligy, S. M. Fahmy, M. A. Mahran and A. A. Hazzaa, Design, synthesis and docking study of pyridine and thieno[2,3-*b*]pyridine derivatives as anticancer PIM-1 kinase inhibitors, *Bioorg. Chem.*, 2018, **80**, 674–692, DOI: **10.1016/j.bioorg.2018.07.024**.

25 CST – HTScan® Pim-1 Kinase Assay Kit, **https://www.cellsignal.com/products/cellular-assay-kits/htscan-pim-1-kinase-assay-kit/7573**, accessed July 17, 2020.

26 M. S. Nafie, K. Arafa, N. K. Sedky, A. A. Alakhdar and R. K. Arafa, Triaryl dicationic DNA minor-groove binders with antioxidant activity display cytotoxicity and induce apoptosis in breast cancer, *Chem.-Biol. Interact.*, 2020, **324**, 109087, DOI: **10.1016/j.cbi.2020.109087**.

27 M. S. Nafie, A. M. Amer, A. K. Mohamed and E. S. Tantawy, Discovery of novel pyrazolo[3,4-b]pyridine scaffold-based derivatives as potential PIM-1 kinase inhibitors in breast cancer MCF-7 cells, *Bioorg. Med. Chem.*, 2020, **28**, 115828, DOI: **10.1016/j.bmc.2020.115828**.

28 E. M. Gad, M. S. Nafie, E. H. Eltamany, M. S. A. G. Hammad, A. Barakat and A. T. A. Boraei, Discovery of New Apoptosis-Inducing Agents for Breast Cancer Based on Ethyl 2-Amino-4,5,6,7-Tetra Hydrobenzo[b]Thiophene-3-Carboxylate: Synthesis, *In Vitro*, and *In Vivo* Activity Evaluation, *Molecules*, 2020, **25**, 2523, DOI: **10.3390/molecules25112523**.

29 M. S. Nafie, S. Mahgoub and A. M. Amer, Antimicrobial and antiproliferative activities of novel synthesized 6-(quinolin-2-ylthio)pyridine derivatives with molecular docking study as multi-targeted JAK2/STAT3 inhibitors, *Chem. Biol. Drug Des.*, 2021, **97**, 553–564, DOI: **10.1111/cbdd.13791**.

30 M. S. Nafie, M. A. Tantawy and G. A. Elmgeed, Screening of different drug design tools to predict the mode of action of steroidal derivatives as anti-cancer agents, *Steroids*, 2019, **152**, 108485, DOI: **10.1016/j.steroids.2019.108485**.

31 M. D. Jacobs, J. Black, O. Futer, L. Swenson, B. Hare, M. Fleming and K. Saxena, Pim-1 Ligand-bound Structures Reveal the Mechanism of Serine/Threonine Kinase Inhibition by LY294002, *J. Biol. Chem.*, 2005, **280**, 13728–13734, DOI: **10.1074/jbc.M413155200**.

32 S. J. Lee, B.-G. Han, J.-W. Cho, J.-S. Choi, J. Lee, H.-J. Song, J. S. Koh and B. I. Lee, Crystal Structure of Pim1 Kinase in Complex with a Pyrido[4,3-D]Pyrimidine Derivative Suggests a Unique Binding Mode, *PLoS One*, 2013, **8**, e70358, DOI: **10.1371/journal.pone.0070358**.

33 V. Asati, D. K. Mahapatra and S. K. Bharti, PIM kinase inhibitors: structural and pharmacological perspectives, *Eur. J. Med. Chem.*, 2019, **172**, 95–108, DOI: **10.1016/j.ejmech.2019.03.050**.

34 K. Li, Y. Li, D. Zhou, Y. Fan, H. Guo, T. Ma, J. Wen, D. Liu and L. Zhao, Synthesis and biological evaluation of quinoline derivatives as potential anti-prostate cancer agents and Pim-1 kinase inhibitors, *Bioorg. Med. Chem.*, 2016, **24**, 1889–1897, DOI: **10.1016/j.bmc.2016.03.016**.